Journal of Photochemistry & Photobiology, A: Chemistry 414 (2021) 113290

Contents lists available at ScienceDirect

Journal of Photochemistry & Photobiology, A: Chemistry

journal homepage: www.elsevier.com/locate/jphotochem

A turn on fluorescent sensor for detecting Al^{3+} and colorimetric detection for Cu^{2+}: Synthesis, cytotoxicity and on-site assay kit

Nur Amira Solehah Pungut [a], Hazwani Mat Saad [b], Kae Shin Sim [b], Kong Wai Tan [a,*]

[a] Department of Chemistry, Faculty of Science, Universiti Malaya, 50603, Kuala Lumpur, Malaysia
[b] Institute of Biological Sciences, Faculty of Science, Universiti Malaya, 50603, Kuala Lumpur, Malaysia

ARTICLE INFO

Keywords:
Rhodamine B
Chemosensors
MTT
Test strips

ABSTRACT

A new rhodamine-fluorene based sensor, RFC has been synthesized for selective detection of Al^{3+} and Cu^{2+} with detection limit as low as 0.12 μM and 1.14 μM respectively. The "off-on'' colorimetric changes of RFC upon binding with the metal ions was differentiated by UV-light. Furthermore, the possible sensing mechanism was proposed from FTIR and ^{1}H NMR spectrum, while the binding stoichiometry was determined from Benesi-Hildebrand and Job's plot. From these studies, a 1:1 stoichiometry of sensor-metal complex for both RFC-Al^{3+} and RFC-Cu^{2+} was recorded. On-site virtual detection of these metal ions by RFC was done by using filter paper as test strips. MTT assay indicated that RFC have no significant cytotoxicity to the cultured human colorectal adenocarcinoma (HT-29) and normal (CCD-18Co) cells.

1. Introduction

Development of fluorogenic and chromogenic chemosensors have been done extensively over the last decade [1–3]. Among the sensors developed, rhodamines-based chemosensors have been preferred ever since the work done back in 1997 [4] owing to its excellent photophysical properties [5]. With the "off-on'' switch mechanism of these chemosensors, rapid detection via naked-eyes could provide both qualitative and quantitative information regarding the analytes detected [6–8] which could be utilized in developing an on-site assay kit [9,10]. Since there is an increasing use of heavy metal ions in the industry, environmental pollution and health hazards are inevitable [11,12]. Although detection of metal ions by conventional methods exists, they are less attractive as compared to chemosensors which are more portable, cost effective and time-efficient [13–15].

In recent years, multitudes of rhodamine-based chemosensors have been developed for detecting multiple metal ions such as Al^{3+} [16,17], Cu^{2+} [18,19], Hg^{2+} [20,21], Fe^{3+} [22,23] and Cr^{3+} [24,25]. Among these metal ions, copper is one of the essential trace elements that plays a major role in sustaining all forms of life and is directly involved in physiological processes of the human body such as copper homeostasis [26,27]. However, surplus amount of copper may lead to ecological pollution and poses health hazards such as, Alzheimer's [28], Menkes [29], and Wilson diseases [30]. On the other hand, being the third most abundant element in the Earth's crust, it's not surprising that aluminium is easily exposed to the general population on the day-to-day basis. Having being used extensively such as in pharmaceuticals [31], automotive [32], textile industry [33], food additive [34] and treatment of water [35], accumulation of excessive amount of this metal would have adverse effects to the environment and human health [36,37]. Deposition of excess aluminium in its ionic state would lead to acidification of soil [38] and known to cause neurodegenerative disease such as Parkinson's disease [39] and kidney damage [40].

Generally, fluorene and its derivatives are known to have high quantum yield making it highly photoluminescence [41,42]. Because of this, it is widely utilized in LEDs [43], two photon absorption [44] and as fluorescent sensors [45,46]. Furthermore, numerous reports have shown a greater detection limit with fluorene based chemosensors [47–50]. Therefore, we have conjugated rhodamine B hydrazide with a fluorene derivative (fluorene-2-carboxaldehyde) in this study.

Herein, the synthesis and characterization of a new rhodamine-fluorene based chemosensor, RFC has been described. Naked eye detection of Al^{3+} and Cu^{2+} by "off-on'' switch mechanism enables rapid detection of these ions by RFC. Furthermore, enhancement of fluorescence emission for Al^{3+} made the detection of the two ions easily distinguishable. Previously, we have reported the synthesis of a fluorescent chemosensor (MEK), obtained from the conjugation of rhodamine B hydrazide and methyl ethyl ketone [51]. Although the sensor

* Corresponding author.
E-mail address: kongwai@um.edu.my (K.W. Tan).

https://doi.org/10.1016/j.jphotochem.2021.113290
Received 25 February 2021; Received in revised form 28 March 2021; Accepted 2 April 2021
Available online 14 April 2021

displayed great detection limit of 8.96 μM (Al^{3+}) and 5.10 μM (Sn^{2+}), detection of Al^{3+} and Cu^{2+} by RFC sensor with fluorene as its conjugate, showed greater detection limit of 0.12 μM and 1.14 μM respectively. Besides, addition of excess EDTA into RFC-metal ion complex shows great reusability of RFC sensor, which is important for practical application. On-site virtual detection of these ions seems promising as test strips have been successfully prepared in aqueous media. The potentiality of RFC in detecting these metal ions in living cells were also studied by conducting MTT assay.

2. Experimental

2.1. Materials and instrumentation

Acetonitrile and chloroform were purchased from MERCK while fluorene-2-carboxaldehyde and Rhodamine B were purchased from Alfa Aesar. The metal ions stock solution was prepared from their chloride, nitrate and sulphate salt. NMR were recorded in deuterated $CDCl_3$ on a JEOL ECX400 MHz instrument. FT-IR spectra were recorded on a Perkin-Elmer Spectrum RX-1 spectrometer using the ATR method. Absorption spectra were measured on a Shimadzu UV-2600 series spectrophotometer. Cary Eclipse fluorescence spectrophotometer was utilized for fluorescence measurements.

2.2. Synthesis of RBH

Rhodamine B hydrazide, RBH was synthesized by following a previous described method [4]. To a (0.5 g, 1.0 mmol) of rhodamine B dissolved in 10 mL of ethanol, an excessive hydrazine hydrate (1.0 mL) was added dropwise. The solution was then refluxed for 6 h until the colour changes from purple to orange. After that, the convection of the solution to room temperature, it was then extracted with hydrochloric acid (HCl) and sodium hydroxide (NaOH). The precipitate formed was then collected and separated by percolation and was washed with 45 mL of distilled water. Finally, the precipitate is left to dry and was then recrystallize with ethanol in a closed conical flask for slow evaporation. The RBH obtained was then characterized by using FTIR, ^{1}H NMR and ^{13}C NMR. Yield = 85 %. ^{1}H NMR (400 MHz, $CDCl_3$-d, s = singlet; d = doublet; t = triplet; q = quadruplet; m = multiplet), δ (ppm): 1.15 (t, 12H, $NCH_2\mathbf{CH_3}$); 3.32 (q, 8H, $N\mathbf{CH_2}CH_3$); 3.60 (s, 2H, NH_2); 6.28 (dd, 2H, Xanthene-H); 6.41 (d, 2H, Xanthene-H); 6.45 (d, 2H, Xanthene-H); 7.09 (m, 1 H); 7.43 (m, 2 H); 7.92 (m, 1 H) (Aromatic-H). **^{13}C NMR** (400 MHz, $CDCl_3$-d), δ (ppm): 12.70 (NCH_2CH_3); 44.45 (NCH_2CH_3); 66.01 (C-N); 98.03, 104.61, 108.10, 123.07, 123.91, 128.18, 130.11, 132.60, 148.96, 151.64, 153.94 (Aromatic-C); 166.24 (C = O).

2.3. Synthesis of RFC

RFC was synthesized by reacting RBH with fluorene-2-carboxaldehyde in ethanol. To a 100 mL flask, rhodamine B hydrazide (0.20 g, 0.4 mmol) was dissolved in 15 mL ethanol, and fluorene-2-carboxaldehyde (0.08 g, 0.4 mmol) was added into the mixture and refluxed for 5 h. The reaction mixture was then concentrated and dried at room temperature. Orange product obtained was then recrystallized with DMF and placed in room temperature for slow evaporation. Yield = 60 %. **^{1}H NMR** (400 MHz, $CDCl_3$-d, s = singlet; d = doublet; t = triplet; q = quadruplet; m = multiplet), δ (ppm): 1.15 (t,12H, NCH_2CH_3); 2.90 (d, 1 H); 3.32 (q, 8 H, NCH_2CH_3); 3.83 (s, 1 H); 6.25 (dd, 2 H); 6.47 (d, 2 H), 6.56 (d, 2 H)(Xanthene-H); 7.11 (dd, 1 H), 7.29 (m, 1 H), 7.48 (m, 4 H), 7.65 (d, 1 H), 7.72 (d, 1 H), 7.81 (s, 1 H), 8.01 (dd, 1 H) (Aromatic-H); 8.58 (s, 1 H, imine-H) **^{13}C NMR** (400 MHz, $CDCl_3$-d, TMS), δ (ppm):12.72 (NCH_2CH_3); 36.83; 44.42 (NCH_2CH_3); 65.96 (C-N); 97.99; 106.05; 108.19; 119.61; 120.26; 123.70; 125.15; 127.16; 128.31; 129.10; 133.42; 134.03; 141.24; 143.36; 144.00; 147.21; 149.05; 152.23 153.09 (Aromatic-C); 165.15 (N-C = O). HRESIMS *m/z* calculated for $C_{42}H_{41}N_4O_2$ $[M+H]^+$ = 632.7998; found = 633.3230. CCDC: 2064878.

2.4. X-ray crystallography

The RFC sensor was crystallized from dimethylformamide (DMF). The crystal data of RFC was analyzed using Oxford Rigaku SuperNova Dual diffractometer equipped with a Mo-Kα X-ray source (λ = 0.71073 Å) with Atlas detector to generate the unit cell parameter and intensity data. Cell refinement, data acquisition and reduction were carried out with CrysAlis Pro software [52]. The structure solution and refinements were done by using SHELXL97 [53]. Crystal visualization was done by using ORTEP3v2 [54] while the crystallographic information was edited and formatted by using publCIF [55].

2.5. Stock solution preparation for spectral detection

A stock solution of RFC (100 mM) was prepared in chloroform. All the metal cations (Ag^+, Al^{3+}, Ca^{2+}, Cd^{2+}, Co^{2+}, Cu^{2+}, La^{3+}, Mn^{2+}, Na^+, Ni^{2+}, Pb^{2+}, Sn^{2+} and Zn^{2+}) of concentration 100 mM was prepared in distilled water. Detection of metal ions solutions are freshly prepared for every spectroscopic measurement.

2.6. UV–vis and fluorescence spectral studies

All experiments were carried out in MeCN/H_2O (9:1, v/v) at pH 7.5 (0.1 mM Tris−HCl buffer). The solvent system of MeCN/H_2O (9:1, v/v) was chosen as it is the optimum condition at which the RFC sensor shows great solubility and sensitivity. To investigate the metal ion selectivity, the test samples were prepared by placing 1 equiv. of the cation stock solution in 3 mL of the RFC solution (50 μM). In the fluorescence measurements (slit: 5.0 nm), excitation was provided at 562 nm and emission was recorded from 550 to 700 nm.

2.7. MTT cytotoxicity assay

The HT-29 (human colorectal adenocarcinoma) and CCD18-Co (normal colon fibroblast) cell lines from American Type Culture Collection (ATCC, USA) were used in current study. The MTT assay was performed as described by Heng et al. [56], with cisplatin as positive control. The data was expressed as mean ± standard deviation of triplicate experiments.

3. Results and discussion

3.1. Synthesis of RFC

RFC sensor was formed through condensation reaction as illustrated in Scheme 1 below. The RFC crystal was grown in DMF solution and was characterized using X-ray crystallography. The molecular structure of RFC can be seen in Fig. 1, where it clearly shows the unique spirolactam ring with the lactam and xanthene moiety forming a vertical plane. The crystal data and structure refinement parameters of RFC are shown in Table S1.

3.2. Spectral studies of RFC using UV–vis and fluorescence spectroscopy

In determining the efficiency of a sensor, the selectivity of RFC (50 μM) towards a series of metal ions (Ag^+, Al^{3+}, Ca^{2+}, Cd^{2+}, Co^{2+}, Cu^{2+}, La^{3+}, Mn^{2+}, Na^+, Ni^{2+}, Pb^{2+}, Sn^{2+} and Zn^{2+}) was investigated using the UV–vis and fluorescence spectroscopy. Upon addition of 1 eq. of Al^{3+} and Cu^{2+} in MeCN/H_2O (9:1, v/v, pH 7.5, Tris−HCl buffer, 0.1 mM), an obvious colour change from colourless to purple was observed, giving rise to the potential of RFC as naked-eye detector for these metal ions. As shown in Fig. 2, upon the coordination of RFC towards Al^{3+} and Cu^{2+}, a peak is observed at 560 nm from the UV–vis spectra, and no peak was observed for the other cations.

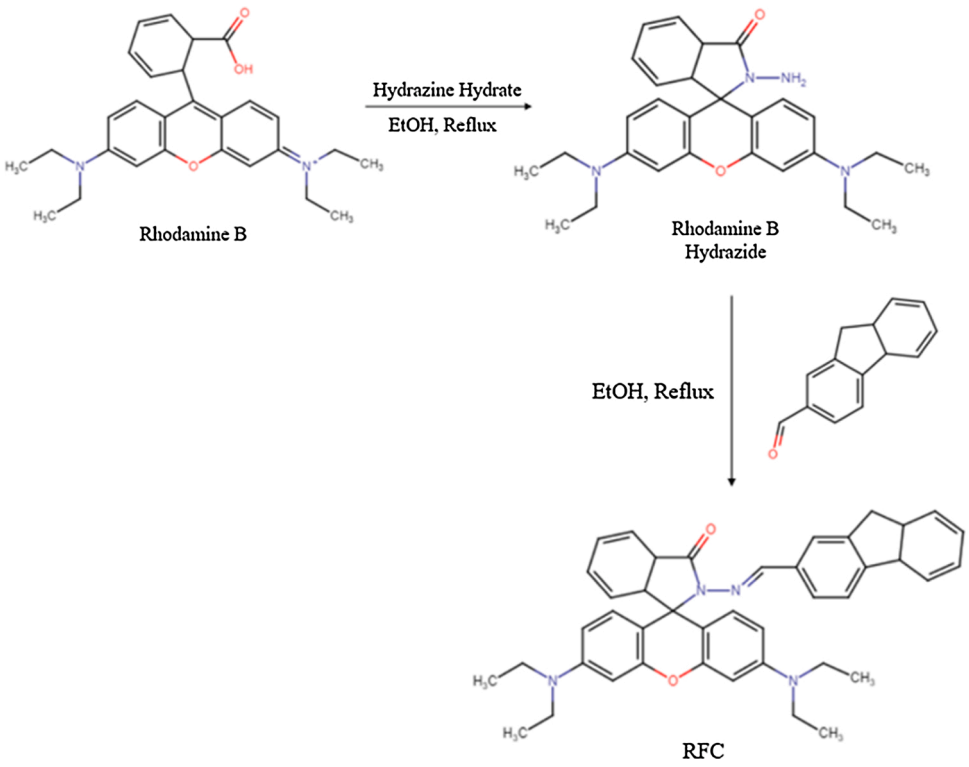

Scheme 1. Synthetic route of RFC.

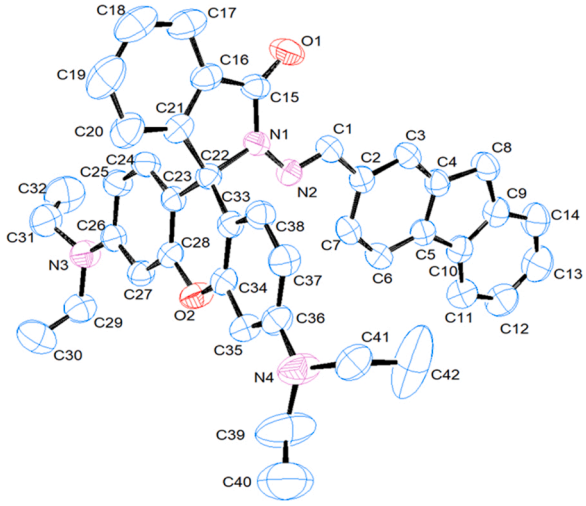

Fig. 1. ORTEP of RFC with atom numbering scheme (50 % thermal ellipsoid probability). Hydrogen atoms were omitted for clarity.

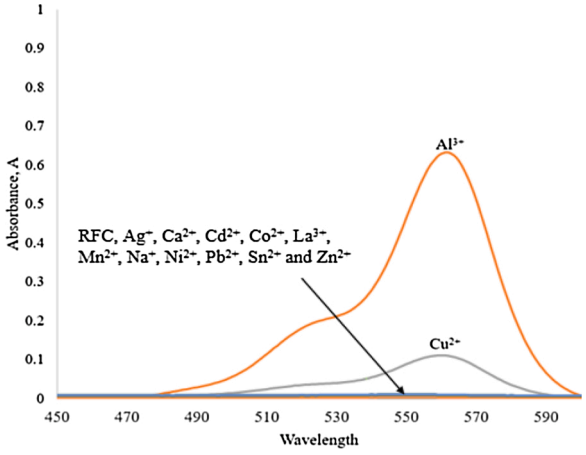

Fig. 2. Absorption changes of RFC (50 μM) upon addition of various metal ions (50 μM) in MeCN/H_2O (9:1, v/v, pH 7.5, Tris−HCl buffer, 0.1 mM).

The fluorogenic behavior of RFC towards the various metal ions was also conducted via the same reaction condition. In the absence of metal ions, a weak band at 588 nm was observed, attributing to the closed spirolactam ring [57] of RFC. When metal ions are added, a strong peak was observed for Al^{3+} and a significantly low peak was observed for Cu^{2+} as depicted in Fig. 4. In Fig. 3b, it could be seen that there is a strong orange fluorescence under the UV lamp which is only observable for Al^{3+}, which is attributed to the opening of the spirolactam ring. Thus, enable an easy and simple method of differentiating Al^{3+} and Cu^{2+} upon detection by RFC sensor.

3.3. Effects of pH

As it is known that for rhodamine derivatives, spirolactam induced-ring opening may occur in acidic condition [58]. Therefore, the effect of pH on the behavior of RFC in detecting Al^{3+} and Cu^{2+} was investigated in MeCN/H_2O (9:1, v/v) solution. Fig. S3 shows that pH value affects the absorbance of RFC towards Al^{3+} and Cu^{2+}. In the absence of metal ions, RFC shows no absorbance from pH 2−11. There are also no changes in absorbance upon binding to Al^{3+} and Cu^{2+} from pH 8−11. Both metal ions show highest absorbance value at pH 7.5, thus the results indicate that detection of RFC towards metal ions is optimum at pH 7.5.

3.4. Titration experiment of RFC

In order to determine the sensitivity of RFC in detecting Al^{3+} and

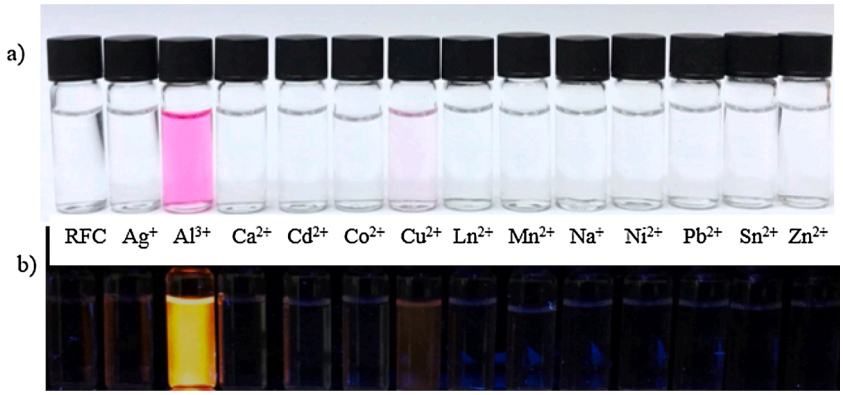

Fig. 3. a) Observed colour change of RFC upon addition of various cations b) Fluorescence change of RFC upon addition of various metal ions under UV-lamp.

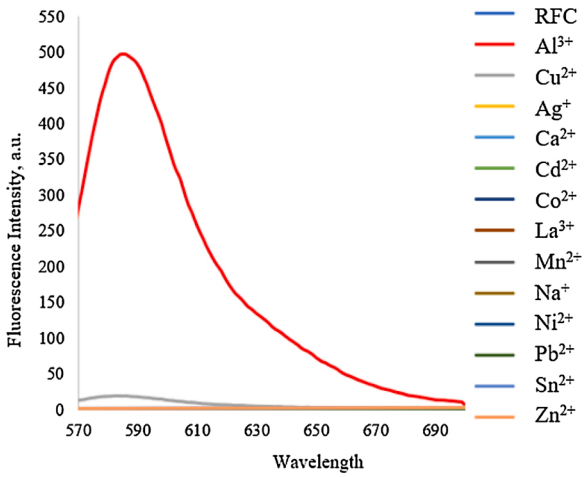

Fig. 4. Fluorescence intensity of RFC (50 μM) upon addition of various cations (50 μM) at λ_{em} = 588 nm.

Cu^{2+}, titration experiment is conducted. Al^{3+} and Cu^{2+} titration against RFC in MeCN/H_2O (9:1, v/v pH 7.5) was monitored using Fluorescence and UV–vis spectra respectively. As shown in Fig. 5a), with increasing concentration of Al^{3+}, the fluorescence intensity at 588 nm increased accordingly. On the other hand, gradual addition of Cu^{2+} causes an increase in the absorbance peak at 560 nm respectively.

From the titration experiments conducted, the limit of detection (LOD) of RFC towards these metal ions were determined. As shown in insets of Fig. 5, linear fitting of the fluorescence and absorbance titration profiles of Al^{3+} and Cu^{2+} were used in determining the LOD respectively. The LOD value of RFC was calculated based on the equation, DL = $3S_d/m$ [59], where S_d is the standard deviation of blank measurement and m is the slope between absorbance intensity and the metal concentration. The detection limit of Al^{3+} and Cu^{2+} was calculated as 0.12 μM and 1.14 μM respectively. These values are much lower than the recommended water quality standard for Al^{3+} (3.71 μM) and Cu^{2+} (20.5 μM), in drinking water by WHO and EPA [60,61]. The LOD comparison of RFC with other reported probes (Table 1) shows its great potency in detecting only Al^{3+} and Cu^{2+} with the ability to discern the two metal ions by means of fluorescent enhancement.

3.5. Association constant calculations

The association constants, K_a of RFC towards Al^{3+} and Cu^{2+} were determined using the Benesi-Hildebrand equations [67,68] as follow

$$\frac{1}{A-A_0} = \frac{1}{K_a(A_{max}-A_0)[Cu^{2+}]} + \frac{1}{A_{max}-A_0} \quad (1)$$

$$\frac{1}{F-F_0} = \frac{1}{K_a(F_{max}-F_0)[Al^{3+}]} + \frac{1}{F_{max}-F_0} \quad (2)$$

A and A_0 is the absorbance of RFC solution in the presence and absence of Cu^{2+} respectively; A_{max} is the saturated absorbance in the presence of excess amount of Cu^{2+}; [Cu^{2+}] is the concentration of metal ions added. While F stands for the fluorescence intensity of RFC towards presence

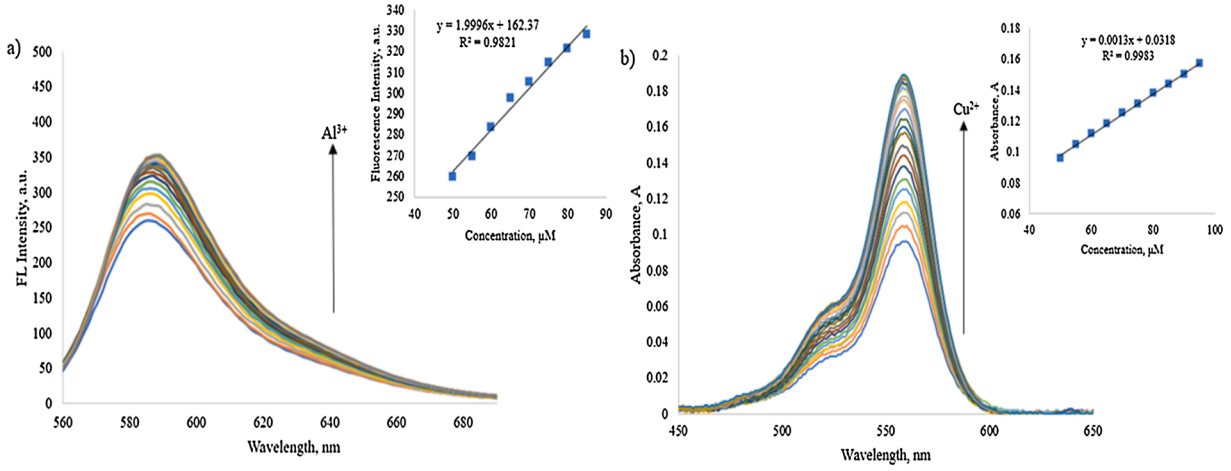

Fig. 5. a) Fluorescence spectrum of Al^{3+} at λ = 588 and b) UV–vis spectrum of Cu^{2+} at λ = 560 nm. Insets: Plot of changes of emission and absorbance intensity with incremental addition of metal ions.

Table 1
Comparison among reported chemosensors with RFC in respect to LOD of Al^{3+} and Cu^{2+}.

Sensor	Detection Method	Chemosensor based	Solvent system	Metal (s) detected	LOD (μM)	Ref.
RD	Fluorescence and Colorimetric	Rhodamine	DMSO/H_2O	CN^- and Cu^{2+}	0.36 (Cu^{2+})	[62]
F3	Fluorescence	Fluorene	MeCN	Cr^{3+} and Al^{3+}	0.31 (Al^{3+})	[63]
L	Fluorescence (Al^{3+} and Cr^{3+} only) and Colorimetric	Rhodamine and azobenzene	EtOH/H_2O	Cu^{2+}, Al^{3+} and Cr^{3+}	1.00 (Cu^{2+}) 2.00 (Al^{3+})	[64]
L1&L2	Fluorescence	Thiazole	MeOH	Al^{3+}	1.00 and 0.75	[65]
1	Fluorescence (Fe^{3+} only) and Colorimetric	Rhodamine	MeOH/H_2O	Cu^{2+}, Al^{3+} and Fe^{3+}	0.29 (Cu^{2+}) 0.01 (Al^{3+})	[66]
RFC (proposed sensor)	Fluorescence (Al^{3+} only) and Colorimetric	Rhodamine and fluorene	MeCN/H_2O	Cu^{2+} and Al^{3+}	1.14 (Cu^{2+}) 0.12 (Al^{3+})	–

and absence of Al^{3+}.

From the equation, by plotting a graph of $1/(F\text{-}F_0)$ or $1/(A\text{-}A_0)$ versus $1/[M^+]$ (Fig. S4 (a) and (b)), a linear regression equation was obtained. Through the slope and intercept, the value of K_a of RFC for Al^{3+} and Cu^{2+} were calculated as 1.83×10^4 M^{-1} and 4.56×10^3 M^{-1} respectively, suggesting that RFC has a higher binding capacity towards Al^{3+} than Cu^{2+}.

3.6. Job's plot

Next, in determining the stoichiometry of RFC with Al^{3+} and Cu^{2+}, Job's plot analysis was conducted. The molar concentration of Al^{3+} and Cu^{2+} ranged from 0 to 1 with a fixed total concentration of RFC + M^{n+} (100 μM) in MeCN/H_2O (9:1, v/v, pH 7.5) at 560 nm. The results revealed that maximum absorbance was achieved at molar fraction of 0.5 for both Al^{3+} (Fig. 6a) and Cu^{2+} (Fig. 6b), indicating that the ratio of RFC- Al^{3+} and RFC- Cu^{2+} complexes as 1:1 (Scheme 2).

3.7. Competitive selectivity of RFC

To further investigate the selectivity of RFC in detecting Al^{3+} and Cu^{2+}, competitive selectivity of RFC (50 μM) in the presence of other cations (Ag^+, Ca^{2+}, Cd^{2+}, Co^{2+}, La^{3+}, Mn^{2+}, Na^+, Ni^{2+}, Pb^{2+}, Sn^{2+} and Zn^{2+}) (50 μM) was studied using fluorescence and UV–vis spectroscopy techniques. From Fig. 7, the recognition of Al^{3+} by RFC is not significantly influenced by other coexisting metal ions. However, in the case of Cu^{2+}, aside from the significantly intensified absorbance in the presence of Al^{3+} (Inset of Fig. 7) the detection of Cu^{2+} by RFC is not affected by other coexisting metal ions.

3.8. Possible binding mechanism

To further elucidate the binding mode of RFC with Al^{3+}, the ^1H NMR titration experiment was carried out. As shown in Fig. 8, during gradual addition of Al^{3+}, the proton of C = N at 8.58 ppm becomes less intense, broadened and shifted downfield, to 8.59 ppm (2 eq. of Al^{3+}) and 8.73 ppm (4 eq. of Al^{3+}). Besides that, decrease in intensities and broadening of peaks were also observed at 6.25 ppm, 6.27 ppm, 6.49 ppm, 6.55 ppm and 6.57 ppm (2 eq. of Al^{3+}) and 6.41 ppm, 6.62 ppm, 6.64 ppm, and 6.70 ppm (4 eq. of Al^{3+}), corresponding to the xanthene protons. The results indicate that the shifts and broadening of peaks are due to the coordination of RFC with Al^{3+}. The complete ^1H NMR spectrum for Fig. 8 could be found in the supplementary material (Fig. S5, S6 and S7).

Due to the paramagnetism of copper, the nuclear magnetic titration was replaced with infrared spectrum (Fig. 9). From the partial IR spectra of RFC sensor, the stretching vibration absorption peaks of C═O and CN═ appeared at 1675 cm^{-1} and 1614 cm^{-1} respectively. Upon binding with Cu^{2+}, the stretching vibration absorption peaks shifted to 1585 cm^{-1}. This shows that both the ketone and amide carbonyl group of RFC are involved in the coordination with Cu^{2+}.

3.9. Reversibility

Reversibility is an essential aspect for a chemical sensor for use in practical application. The reversibility of RFC towards target analytes (Al^{3+} and Cu^{2+}) was tested by using EDTA. As depicted in Fig. S8a, upon addition of excessive amount of EDTA into the RFC + Al^{3+} system, decolourization of the solution occurs immediately (Fig. 10) followed by the disappearance of absorbance peak at 560 nm. Subsequent addition of Al^{3+} into the system shows the recovery of the absorbance peak and the solution changes back to purple colour. The same method was applied for Cu^{2+} (Fig. S8b) with repeatability of up to 10 times and up to 12 times for Al^{3+} (Fig. S8a).

3.10. On site assay study

In order to test the potential of RFC for practical application, a paper based on-site visual detection of Al^{3+} and Cu^{2+} by using the common filter paper have been prepared. The test strips were prepared by soaking the filter paper into RFC (25 mM) solution for 5 min and left to dry in air. It was then used to detect different concentration of Al^{3+} and Cu^{2+} in aqueous media. As seen in Fig. 11a and b, it shows a gradual increase in

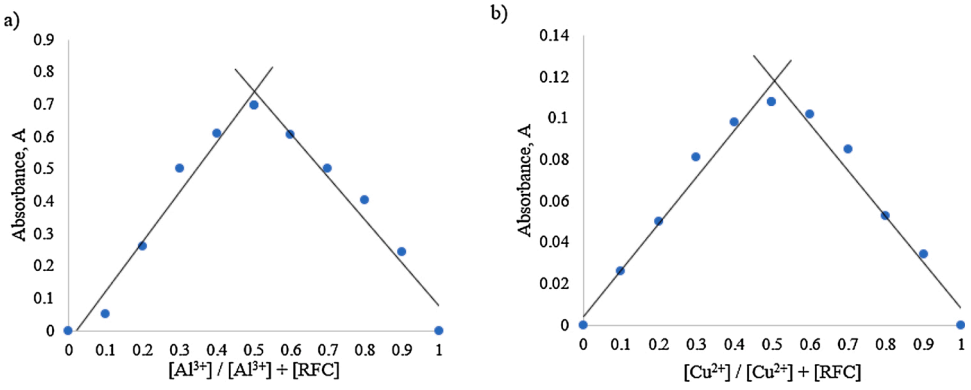

Fig. 6. Job's plot of RFC and M^{n+} ($[M^{n+}]$ + [RFC] =100 μM) at λ = 560 nm for a) Al^{3+} and b) Cu^{2+} at 560 nm.

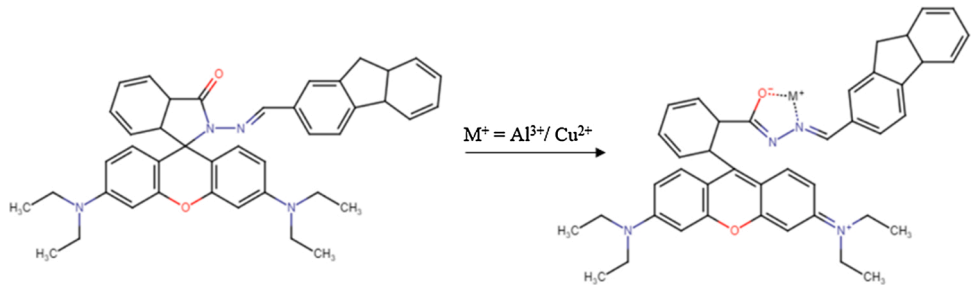

Scheme 2. Proposed binding mechanism of RFC with Al^{3+} and Cu^{2+}.

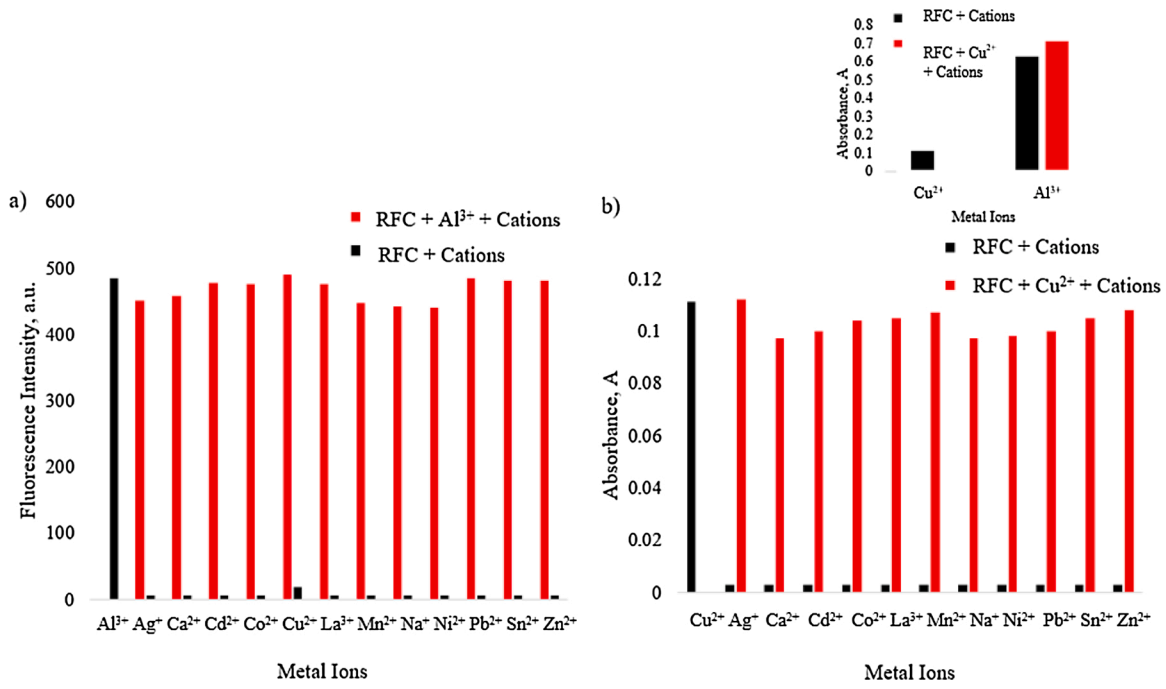

Fig. 7. The competitive selectivity of RFC (50 μM) based on changes in fluorescence intensity for a) Al^{3+} at 588 nm and absorbance changes for b) Cu^{2+} at 560 nm in the presence of various cations (50 μM). Inset: Absorbance changes for Cu^{2+} in the presence of Al^{3+}.

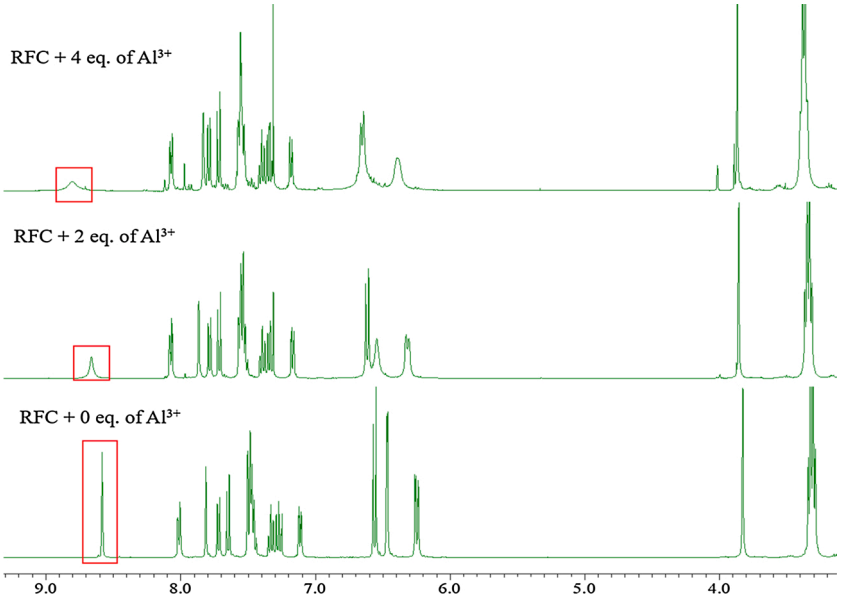

Fig. 8. ^{1}HNMR spectral changes of RFC upon addition of Al^{3+} in $CDCl_3$-d.

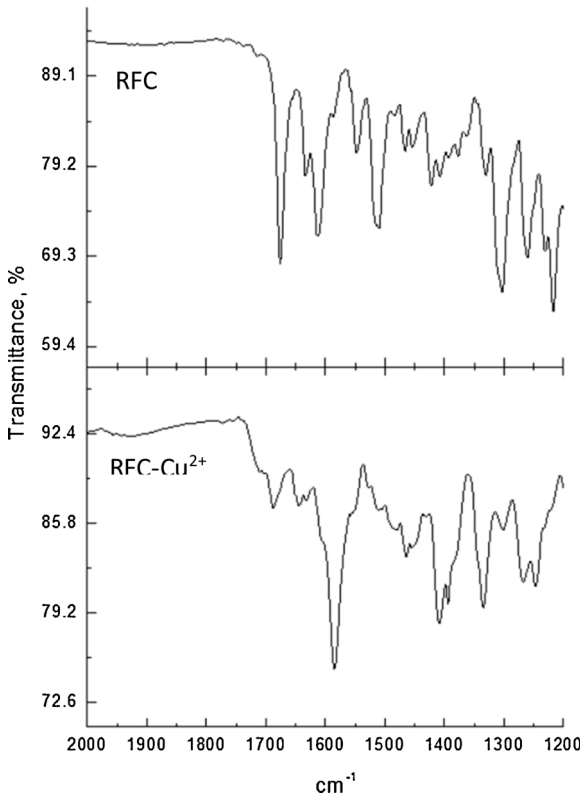

Fig. 9. Infrared spectra of RFC and RFC-Cu^{2+} complex.

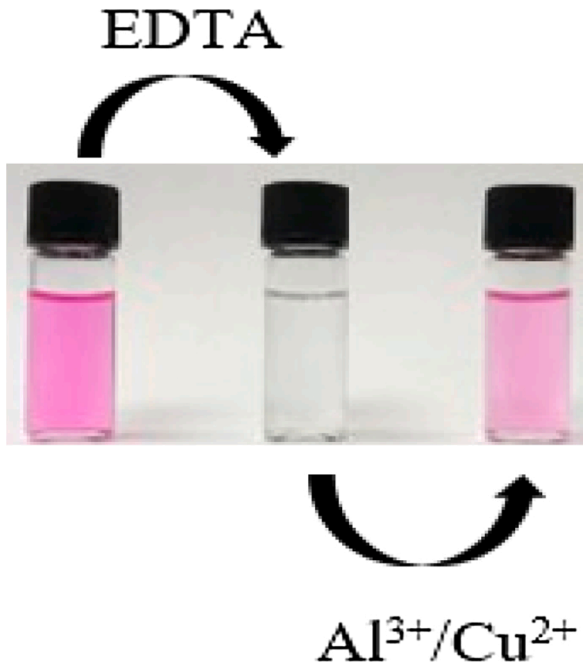

Fig. 10. Colorimetric changes upon addition of EDTA and re-addition of metal ions.

pink intensity of the test strips upon increasing concentration of ions from 0 to 500 μM. By placing the test strips under the UV-lamp, the two metal ions are easily distinguishable by appearance of bright orange fluorescence for Al^{3+} (Fig. 11c). These results show great applicability of the test strips in detecting these metal ions in real water sample.

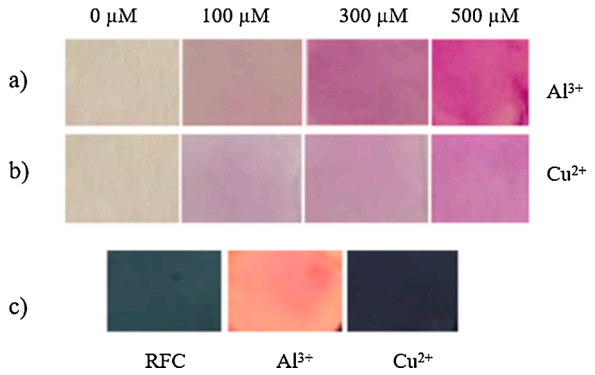

Fig. 11. Colorimetric changes of test strips upon addition of increasing metal ions for a) Al^{3+} and b) Cu^{2+} c) Changes in test-strips under the UV-lamp.

3.11. *In vitro cell growth inhibitory effects of the RFC*

To evaluate the cytotoxicity of RFC sensor, cell viability was determined by MTT assay conducted on the human colorectal adenocarcinoma (HT-29) and normal (CCD-18Co) cell lines with cisplatin as the positive control (Table S2). As depicted in Fig. 12, at least 58 % of the CCD-18Co cells and 47 % of HT-29 cells remained alive after incubation for 72 h with RFC. On the other hand, at the highest concentration, the cell viability was less than 20 % when both cells were treated with cisplatin. Thus, the results suggest that RFC could be used to detect Al^{3+} and Cu^{2+} in biological samples.

4. Conclusion

In summary, the current study reported a new rhodamine-based chemosensor, RFC for simultaneous detection of Al^{3+} and Cu^{2+}. Not only does RFC shows an "off-on'' colorimetric changes via naked-eye detection, it is also able to differentiate between the two metal ions under the UV-lamp. Furthermore, RFC shows great sensitivity in

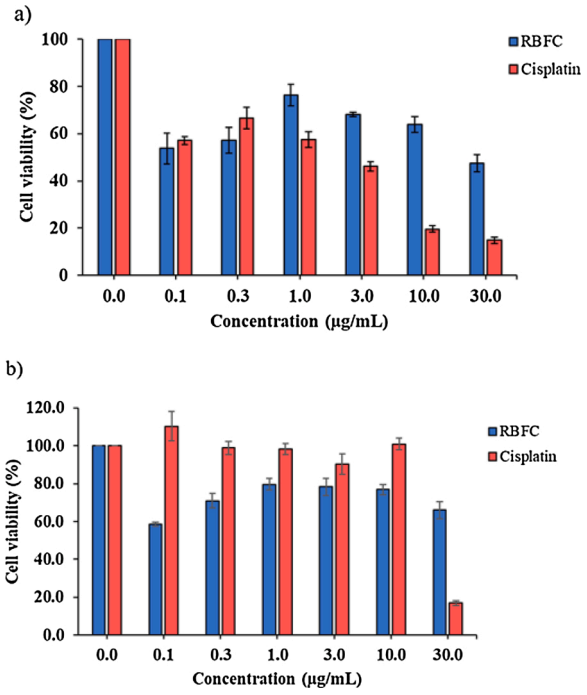

Fig. 12. Cytotoxic activity of RFC against HT-29 (a) and CCD-18Co (b) cell lines. Cisplatin was used as positive control. Data is expressed as mean ± SD (n = 3). *$p < 0.05$ indicates significant different from untreated control.

detecting Al^{3+} and Cu^{2+} in an effective concentration as low as 0.23 μM and 1.12 μM respectively. Not only that, the reusability of the sensor was achieved and proven by adding excess EDTA into the solution containing RFC-Metal ions. By conducting the on-site assay study, the results suggest great potentiality in detecting Al^{3+} and Cu^{2+} for environmental use as it provides a rather simple, convenient, and effective method.

Author statement

Nur Amira Solehah Pungut: Writing- original draft, Validation, Investigation, Visualization, Data curation, Methodology, Conceptualization, **Hazwani Mat Saad**: Methodology, Investigation, Validation, **Kae Shin Sim**: Writing - review & editing, **Kong Wai Tan**: Writing – review & editing, Supervision

Declaration of Competing Interest

The authors declare that they have no known competing financial interests or personal relationships that could have appeared to influence the work reported in this paper.

Acknowledgements

This research was supported by Ministry of Higher Education for the grant provided (FRGS/1/2019/STG01/UM/02/11) in completing the project, and the collaboration of Ministry of Education and Universiti Malaysia Sabah (UMS) for the scholarship provided. Special thanks to Dr. Low Yun Yee for the mass spectrum data.

Appendix A. Supplementary data

Supplementary material related to this article can be found, in the online version, at doi:https://doi.org/10.1016/j.jphotochem.2021.113290.

References

[1] D. Jiang, X. Xue, G. Zhang, Y. Wang, H. Zhang, C. Feng, Z. Wang, H. Zhao, Simple and efficient rhodamine-derived VO2+ and Cu2+-responsive colorimetric and reversible fluorescent chemosensors toward the design of multifunctional materials, J. Mater. Chem. C. 7 (2019) 3576–3589.
[2] X. Wang, T. Li, A novel "off-on" rhodamine-based colorimetric and fluorescent chemosensor based on hydrolysis driven by aqueous medium for the detection of Fe3+, Spectrochim. Acta, Part A. 229 (2020), 117951.
[3] M. Dong, T.H. Ma, A.J. Zhang, Y.M. Dong, Y.W. Wang, Y. Peng, A series of highly sensitive and selective fluorescent and colorimetric "off-on" chemosensors for Cu (II) based on rhodamine derivatives, Dyes Pigm. 87 (2010) 164–172.
[4] V. Dujols, F. Ford, A.W. Czarnik, A long-wavelength fluorescent chemodosimeter selective for Cu(II) ion in water, J. Am. Chem. Soc. 119 (1997) 7386–7387.
[5] C. Albrecht, Joseph R. Lakowicz, Principles of Fluorescence Spectroscopy, 3rd edition, 390, Anal. Bioanal. Chem., 2008, pp. 1223–1224.
[6] P. Milindanuth, P. Pisitsak, A novel colorimetric sensor based on rhodamine-B derivative and bacterial cellulose for the detection of Cu(II) ions in water, Mater. Chem. Phys. 216 (2018) 325–331.
[7] R. Sheng, P. Wang, Y. Gao, Y. Wu, W. Liu, J. Ma, H. Li, S. Wu, Colorimetric test kit for Cu2+ detection, Org. Lett. 10 (2008) 5015–5018.
[8] J.W. Jeong, B.A. Rao, Y.A. Son, Rhodamine-chloronicotinaldehyde-based "OFF–ON" chemosensor for the colorimetric and fluorescent determination of Al3+ ions, Sens. Actuators, B. 208 (2015) 75–84.
[9] V.K. Gupta, N. Mergu, L.K. Kumawat, A new multifunctional rhodamine-derived probe for colorimetric sensing of Cu(II) and Al(III) and fluorometric sensing of Fe (III) in aqueous media, Sens. Actuators, B. 223 (2016) 101–113.
[10] L. Liu, H. Lin, Paper-based colorimetric array test strip for selective and semiquantitative multi-ion analysis: simultaneous detection of Hg2+, Ag+, and Cu2+, Anal. Chem. 86 (2014) 8829–8834.
[11] A. Lenart-Boroń, P. Boroń, The effect of industrial heavy metal pollution on microbial abundance and diversity in soils—a review, in: environ, Risk Assess. Soil Contam. (2014).
[12] A.S. Mohammed, A. Kapri, R. Goel, Heavy metal pollution: source, impact, and remedies. Biomanagement of Metal-contaminated Soils, Springer, 2011, pp. 1–28.
[13] L. Ma, T. Leng, K. Wang, C. Wang, Y. Shen, W. Zhu, A coumarin-based fluorescent and colorimetric chemosensor for rapid detection of fluoride ion, Tetrahedron 73 (2017) 1306–1310.
[14] Y. Zhou, J. Zhang, L. Zhang, Q. Zhang, T. Ma, J. Niu, A rhodamine-based fluorescent enhancement chemosensor for the detection of Cr3+ in aqueous media, Dyes Pigm. 97 (2013) 148–154.
[15] K. Van Meel, A. Smekens, M. Behets, P. Kazandjian, R. Van Grieken, Determination of platinum, palladium, and rhodium in automotive catalysts using high-energy secondary target X-ray fluorescence spectrometry, Anal. Chem. 79 (2007) 6383–6389.
[16] Z. Li, Q. Hu, C. Li, J. Dou, J. Cao, W. Chen, Q. Zhu, A 'turn-on' fluorescent chemosensor based on rhodamine-N-(3-aminopropyl)-imidazole for detection of Al3+ ions, Tetrahedron Lett. 55 (2014) 1258–1262.
[17] R. Kaur, S. Saini, N. Kaur, N. Singh, D.O. Jang, Rhodamine-based fluorescent probe for sequential detection of Al3+ ions and adenosine monophosphate in water, Spectrochim. Acta, Part A. 225 (2020), 117523.
[18] F.J. Huo, J. Su, Y.Q. Sun, C.X. Yin, H.B. Tong, Z.X. Nie, A rhodamine-based dual chemosensor for the visual detection of copper and the ratiometric fluorescent detection of vanadium, Dyes Pigm. 86 (2010) 50–55.
[19] Y. Jiao, L. Zhou, H. He, J. Yin, Q. Gao, J. Wei, C. Duan, X. Peng, A novel rhodamine B-based "off-on'' fluorescent sensor for selective recognition of copper (II) ions, Talanta 184 (2018) 143–148.
[20] X. Zeng, L. Dong, C. Wu, L. Mu, S.-F. Xue, Z. Tao, Highly sensitive chemosensor for Cu(II) and Hg(II) based on the tripodal rhodamine receptor, Sens. Actuators, B. 141 (2009) 506–510.
[21] T. Rasheed, C. Li, Y. Zhang, F. Nabeel, J. Peng, J. Qi, L. Gong, C. Yu, Rhodamine-based multianalyte colorimetric probe with potentialities as on-site assay kit and in biological systems, Sens. Actuators, B. 258 (2018) 115–124.
[22] A. Pipattanawarothai, T. Trakulsujaritchok, Hybrid polymeric chemosensor bearing rhodamine derivative prepared by sol-gel technique for selective detection of Fe3+ ion, Dyes Pigm. 173 (2020), 107946.
[23] F. Zhou, T.H. Leng, Y.J. Liu, C.Y. Wang, P. Shi, W.H. Zhu, Water-soluble rhodamine-based chemosensor for Fe3+ with high sensitivity, selectivity and anti-interference capacity and its imaging application in living cells, Dyes Pigm. 142 (2017) 429–436.
[24] O. Sunnapu, N.G. Kotla, B. Maddiboyina, G.S. Asthana, J. Shanmugapriya, K. Sekar, S. Singaravadivel, G. Sivaraman, Rhodamine based effective chemosensor for Chromium(III) and their application in live cell imaging, Sens. Actuators, B. 246 (2017) 761–768.
[25] A.J. Weerasinghe, A.N. Oyeamalu, F.A. Abebe, A.R. Venter, E. Sinn, Rhodamine based turn-on sensors for Ni2+ and Cr3+ in organic media: detecting CN− via the metal displacement approach, J. Fluoresc. 26 (2016) 891–898.
[26] J.J.A. Cotruvo, A.T. Aron, K.M. Ramos-Torres, C.J. Chang, Synthetic fluorescent probes for studying copper in biological systems, Chem. Soc. Rev. 44 (2015) 4400–4414.
[27] J.S. Valentine, P.A. Doucette, S. Zittin Potter, Copper-zinc superoxide dismutase and amyotrophic lateral sclerosis, Annu. Rev. Biochem. 74 (2005) 563–593.
[28] D. Strausak, J.F.B. Mercer, H.H. Dieter, W. Stremmel, G. Multhaup, Copper in disorders with neurological symptoms: Alzheimer's, Menkes, and Wilson diseases, Brain Res. Bull. 55 (2001) 175–185.
[29] M. DiDonato, B. Sarkar, Copper transport and its alterations in Menkes and Wilson diseases, Biochim. Biophys. Acta, Mol. Basis Dis. 1360 (1997) 3–16.
[30] R. Seth, S. Yang, S. Choi, M. Sabean, E.A. Roberts, In vitro assessment of copper-induced toxicity in the human hepatoma line, Hep G2, Toxicol. In Vitro 18 (2004) 501–509.
[31] C.M. Reinke, J. Breitkreutz, H. Leuenberger, Aluminium in over-the-counter drugs, Drug Saf. 26 (2003) 1011–1025.
[32] W.S. Miller, L. Zhuang, J. Bottema, A.J. Wittebrood, P. De Smet, A. Haszler, A. Vieregge, Recent development in aluminium alloys for the automotive industry, Mater. Sci. Eng., A. 280 (2000) 37–49.
[33] G. Ciardelli, N. Ranieri, The treatment and reuse of wastewater in the textile industry by means of ozonation and electroflocculation, Water Res. 35 (2001) 567–572.
[34] S.M. Saiyed, R.A. Yokel, Aluminium content of some foods and food products in the USA, with aluminium food additives, Food Addit. Contam. 22 (2005) 234–244.
[35] P.T. Srinivasan, T. Viraraghavan, K.S. Subramanian, Aluminium in drinking water: an overview, Water Sa 25 (1999) 47–55.
[36] O. Momot, B. Synzynys, Toxic aluminium and heavy metals in groundwater of middle Russia: health risk assessment, Int. J. Environ. Res. Public Health 2 (2005).
[37] B.O. Rosseland, T.D. Eldhuset, M. Staurnes, Environmental effects of aluminium, Environ. Geochem. Health 12 (1990) 17–27.
[38] W. Barabasz, D. Albinska, M. Jaskowska, J. Lipiec, Ecotoxicology of aluminium, Pol. J. Environ. Stud. 11 (2002) 199–203.
[39] B. Halliwell, Oxidants and the central nervous system: some fundamental questions. Is oxidant damage relevant to Parkinson's disease, Alzheimer's disease, traumatic injury or stroke? Acta Neurol. Scand. 80 (1989) 23–33.
[40] D.R. Burwen, S.M. Olsen, L.A. Bland, M.J. Arduino, M.H. Reid, W.R. Jarvis, Epidemic aluminum intoxication in hemodialysis patients traced to use of an aluminum pump, Kidney Int. 48 (1995) 469–474.
[41] W.Y. Wong, C.L. Ho, Di-, oligo- and polymetallaynes: syntheses, photophysics, structures and applications, Coord. Chem. Rev. 250 (2006) 2627–2690.
[42] J.C. Sanchez, W.C. Trogler, Efficient blue-emitting silafluorene–fluorene-conjugated copolymers: selective turn-off/turn-on detection of explosives, J. Mater. Chem. 18 (2008) 3143–3156.
[43] M.T. Bernius, M. Inbasekaran, J. O'Brien, W. Wu, Progress with light-emitting polymers, Adv. Mater. 12 (2000) 1737–1750.
[44] S. Oger, D. Schapman, R. Mougeot, S. Leleu, N. Lascoux, P. Baldeck, M. Benard, T. Gallavardin, L. Galas, X. Franck, Two-photon absorption and cell imaging of

fluorene-functionalized epicocconone analogues, Chem. - Eur. J. 25 (2019) 10954–10964.
[45] J.L. Pablos, S. Ibeas, A. Muñoz, F. Serna, F.C. García, J.M. García, Solid polymer and metallogel networks based on a fluorene derivative as fluorescent and colourimetric chemosensors for Hg(II), React. Funct. Polym. 79 (2014) 14–23.
[46] G. Zhao, Y. Sun, H. Duan, Four xanthene–fluorene based probes for the detection of Hg2+ ions and their application in strip tests and biological cells, New J. Chem. 45 (2021) 685–695.
[47] F. dos Santos Carlos, M.C. Nunes, L. De Boni, G.S. Machado, F.S. Nunes, A novel fluorene-derivative schiff-base fluorescent sensor for copper(II) in organic media, J. Photochem. Photobiol., A. 348 (2017) 41–46.
[48] A. Dhara, A. Jana, S. Konar, S.K. Ghatak, S. Ray, K. Das, A. Bandyopadhyay, N. Guchhait, S.K. Kar, A novel rhodamine-based colorimetric chemodosimeter for the rapid detection of Al3+ in aqueous methanol: fluorescent 'OFF–ON' mechanism, Tetrahedron Lett. 54 (2013) 3630–3634.
[49] K.D. Belfield, M.V. Bondar, A. Frazer, A.R. Morales, O.D. Kachkovsky, I. A. Mikhailov, A.E. Masunov, O.V. Przhonska, Fluorene-based metal-ion sensing probe with high sensitivity to Zn2+ and efficient two-photon absorption, J. Am. Chem. Soc. 114 (2010) 9313–9321.
[50] K.S. Min, R. Manivannan, Y.A. Son, Rhodamine-fluorene based dual channel probe for the detection of Hg2+ ions and its application in digital printing, Sens. Actuators, B. 261 (2018) 545–552.
[51] P.W. Cheah, M.P. Heng, A. Izati, C.H. Ng, K.W. Tan, Rhodamine B conjugate for rapid colorimetric and fluorimetric detection of aluminium and tin ions and its application in aqueous media, Inorg. Chim. Acta. 512 (2020), 119901.
[52] Oxford Diffraction, Crys Alis PRO, Oxford Diffraction Ltd, Yarnton, England, 2009.
[53] G.M. Sheldrick, SHELXL and SHELXS, Acta Crystallogr., Sect. A: Found. Crystallogr. 64 (2008) 112.
[54] L.J. Farrugia, ORTEP-3 for windows-a version of ORTEP-III with a graphical user interface (GUI), J. Appl. Crystallogr. 30 (1997) 565.
[55] S.P. Westrip, publCIF: software for editing, validating and formatting crystallographic information files, J. Appl. Crystallogr. 43 (2010) 920–925.
[56] M.P. Heng, C.H. Tan, H.M. Saad, K.S. Sim, K.W. Tan, Mitochondria-dependent apoptosis inducer: Testosterone-N4-ethylthiosemicarbazonate and its metal complexes with selective cytotoxicity towards human colorectal carcinoma cell line (HCT 116), Inorg. Chim. Acta. 507 (2020), 119581.
[57] H.N. Kim, M.H. Lee, H.J. Kim, J.S. Kim, J. Yoon, A new trend in rhodamine-based chemosensors: application of spirolactam ring-opening to sensing ions, Chem. Soc. Rev. 37 (2008) 1465–1472.
[58] X. Chen, T. Pradhan, F. Wang, J.S. Kim, J. Yoon, Fluorescent chemosensors based on spiroring-opening of Xanthenes and related derivatives, J. Am. Chem. Soc. 112 (2012) 1910–1956.
[59] A. Shrivastava, V. Gupta, Methods for the determination of limit of detection and limit of quantitation of the analytical methods, Chron. Young Sci. 2 (2011) 21.
[60] WHO, Aluminium in Drinking-water: Background Document for Development of WHO Guidelines for Drinking-water Quality, 2003.
[61] D.J. Fitzgerald, Safety guidelines for copper in water, Am. J. Clin. Nutr. 67 (1998) 1098S–1102S.
[62] C. Long, J. Hu, Q.Q. Fu, P.W. Ni, A new colorimetric and fluorescent probe based on Rhodamine B hydrazone derivatives for cyanide and Cu2+ in aqueous media and its application in real life, Spectrochim. Acta, Part A. 219 (2019) 297–306.
[63] M. Tajbakhsh, G.B. Chalmardi, A. Bekhradnia, R. Hosseinzadeh, N. Hasani, M. A. Amiri, A new fluorene-based schiff-base as fluorescent chemosensor for selective detection of Cr3+ and Al3+, Spectrochim. Acta, Part A. 189 (2018) 22–31.
[64] S. Mabhai, M. Dolai, S.K. Dey, A. Dhara, S.M. Choudhury, B. Das, S. Dey, A. Jana, Rhodamine-azobenzene based single molecular probe for multiple ions sensing: Cu (2+), Al(3+), Cr(3+) and its imaging in human lymphocyte cells, Spectrochim. Acta, Part A. 219 (2019) 319–332.
[65] V.K. Gupta, A.K. Singh, L.K. Kumawat, Thiazole Schiff base turn-on fluorescent chemosensor for Al3+ ion, Sens. Actuators, B. 195 (2014) 98–108.
[66] Q. Hu, Y. Liu, Z. Li, R. Wen, Y. Gao, Y. Bei, Q. Zhu, A new rhodamine-based dual chemosensor for Al3+ and Cu2+, Tetrahedron Lett. 55 (2014) 4912–4916.
[67] H.A. Benesi, J.H. Hildebrand, A spectrophotometric investigation of the interaction of iodine with aromatic hydrocarbons, J. Am. Chem. Soc. 71 (1949) 2703–2707.
[68] K.C. Tayade, A.S. Kuwar, U.A. Fegade, H. Sharma, N. Singh, U.D. Patil, S. B. Attarde, Design and synthesis of a pyridine based chemosensor: highly selective fluorescent probe for Pb2+, J. Fluoresc. 24 (2014) 19–26.